IEEE Access
Multidisciplinary | Rapid Review | Open Access Journal

Received 13 September 2022, accepted 21 September 2022, date of publication 12 October 2022, date of current version 20 October 2022.

Digital Object Identifier 10.1109/ACCESS.2022.3213948

RESEARCH ARTICLE

Performance Analysis of Renewable Energy Based Distributed Generation System Using ANN Tuned UPQC

NOOR ZANIB[1], MUNIRA BATOOL[2], SALEEM RIAZ[3], AND FAWAD NAWAZ[2]

[1]Department of Electrical Engineering, University of Engineering and Technology, Taxila 47050, Pakistan
[2]Engineering Institute of Technology, Perth, WA 6005, Australia
[3]School of Automation, Northwestern Polytechnical University, Xi'an, Shaanxi 170072, China

Corresponding author: Saleem Riaz (saleemriaznwpu@mail.nwpu.edu.cn)

This work was supported in part by the Engineering Institute of Technology.

ABSTRACT Emerging trends and advances in techniques in power electronics, Unified Power Quality Conditioner (UPQC) has a superior performance compared to other methods. The paper proposes the application of a ANN based UPQC to enhance the power quality of a three-phase Low-voltage network connected to a hybrid distribution generation (DG) system. The proposed work emphases the detailed performance analysis of a distributed generation system that integrates a solar PV and wind energy system by utilizing Unified Power Quality Conditioner (UPQC) with an artificial neural network (ANN) controller with respect to proportional-integral (PI) controller. The core objective of the proposed ANN is to offer good steady and dynamic state performance compared to the PID controller. The system called UPQC-ANN-RE feeds energy generated by a photovoltaic array and a wind turbine into the electrical grid and loads attached to a system of 3-phase 4-wire electrical distribution. In addition to inserting active/real power in the utility grid, the system of UPQC-ANN-RE functions as a UPQC, improving power quality signs e.g., voltage and current harmonics and power factor. A detailed analysis of the active-real power flow by converters is carried out to allow a good understanding of the operation of the UPQC-ANN-RE. The simulation outcomes are presented to assess the dynamic and steady state performance of the system of UPQC-ANN-RE connected to an electrical distribution system and to compare the consequences with the PI controller.

INDEX TERMS Distributed generation system, unified power quality conditioner, artificial neural network, power quality, renewable energy sources.

NOMENCLATURE

C_{dc}	DC-bus equivalent capacitance
C_{pa}	Capacitive filters (parallel NPC inverter)
C_{pwm}	PWM gain
f_s	Utility grid frequency
$i_{pv-wind}$	PV and Wind turbine Current
i_{dc}	ANN controller DC link voltage output signal
i_{ff}	Feed forward current
i_L	Load current
i_{pac}	Parallel NPC inverter current
i_s	Grid current
L_{pac}	inductive Filters (parallel NPC inverter)
L_{sec}	Inductive filters (series NPC inverter)
L_T	Leakage inductance of series coupling transformers
n_T	Turn ratio of the series transformer
$P_{pv-wind}$	Active power generated through the PV array and Wind turbine
P_L	Active load power
P_{pac}	Active power of NPC parallel inverter
P_{sec}	Active Power of NPC series inverter
R_{pac}	Internal resistances of the parallel NPC inverter inductors
R_{sec}	Internal resistances of the series NPC inverter inductors
R_T	Resistances of series coupling transformers
S_L	Apparent power of Load

The associate editor coordinating the review of this manuscript and approving it for publication was Yilun Shang.

$v^*_{dc_{max}}$	Maximum dc-bus voltage
$v^*_{dc_{min}}$	Minimum dc-bus voltage
V_{dc}	DC-bus voltage
V_L	RMS Load Voltages
V_s	RMS Grid Voltage
3P4W	Three phase four wire
ANN	Artificial Neural Network
DGs	Distributed generation systems
DVR	Dynamic voltage restorer
ESS	Energy Storage Systems
FACTS	Flexible AC transmission system controllers
LMBP	Levenberg-Marquardt backpropagation
MPPT	Maximum Power Point Tracking
NPC	Neutral Point Clamped
P&O	Perturbs and Observes
P-APF	Shunt active power filter
PCC	Point of common coupling
PF	Power Factor
PI	Proportional-Integral
PLL	
PMSG	Permanent Magnetic Synchronous Generator
PQ	Power Quality
PV	Photovoltaics
RE	Renewable energy
RES	Renewable energy sources
S-APF	Series active power filter
STATCOM	Static synchronous compensator
STC	Standard test conditions
THD	Total Harmonic Distortion
UPFC	Unified power flow controller
UPQC	Unified Power Quality Conditioner
WE	Wind Energy

I. INTRODUCTION

In latest years, severe socio-economic issues and ecological effects because of the building of latest and huge power plants (nuclear and hydroelectric) along with the building of power plants based upon the fossil fuels (oil, natural gas, coal, and others) have provoked managements and scholars around the world to pursue alternative way out and schemes to meet the rising demand for energy. In this perspective, the production of electricity from alternate and ''hybrid-renewable-energy system'' (HRES) plays a vital role in increasing the long-term energy supply. A hybrid system can address and overcome the limitations of renewable energy resources with efficiency, reliability, and economics. Therefore, in addition to reducing violent environmental influences, this situation permits for an increasing divergence of energy matrix which injected in present framework of electricity production. Several researchers presented HRES models including renewable energies such as wind-biomass, hydro-solar, wind-PV-hydro, PV-biomass or wind-PV-biomass, to plan a power plant in stand-alone or grid-connected modes. Hence, renewable energy sources (RES) based distributed generation systems (DGs) such as wind and solar power have emerged as a vital and modern way out that can be integrated into traditional energy production systems [1], [2], [3], [4], [5]. On the other hand, its integration requires numerous power electronic devices e.g., converters, inverters, etc., which alternatively reduce the quality of the power both on source and load side. Apart from this, the use of non-linear loads at the point of common coupling (PCC) also inserts the harmonics in system. Relatively common PQ problems are voltage sags/swells, flicker and harmonics [6], [7], [8], [9].

With the need for clean energy, in addition to the rigorous power quality desires of sophisticated loads and power electronics devices, here is a requirement for multifunctional systems capable of integrating clean energy production and improving the quality of power. In [10] and [11], a 3-Φ multifunctional solar power conversion system that recompenses the load-side PQ problems has been proposed. In [12] and [13], a 1-Φ photovoltaic solar inverter has been proposed with an active power filtering ability. Because of the increasing spread of renewable energy sources, the use of DGs is becoming increasingly popular. However, the primary function of the DGs is to feed active power into the grid, its multifunctionality can be extended to comprise active/real power-line conditioning functions. In this state, at the same time the integrated DGS may do active power line compensation in addition to power generation and thus help improve PQ indicators [14], [15], [16], [17], [18], [19], [20], [21]. To alleviate PQ events passive filters, active filters, and flexible AC transmission system controllers (FACTS) are commonly utilized. Passive filters attenuate harmonics individually and are bulky inherently. Active filters are using to lessen harmonics and recompense reactive power. However, they are costly than passive filters. Numerous FACTS controllers are too utilized to enhance performance and power quality [6], [22], [23]. FACTS devices, including UPFC-FLC, UPFC, SVC, UPQC and GUPFC are the most widely used power quality enhancement devices. The employment of FACT devices solves the voltage stability problem while improving the power quality of the grid [24], [25], [26], [27]. The improvement of the grid stability and the decrease in the THD has been obtained by applying the STATCOM in relation to the ESS [24]. Likewise, the wind power production system experiences THD and unstable voltage. So, STATCOM has also been applied with the grid-tied wind energy (WE) system [25]. In [26], an integrated solar photovoltaic system with a dynamic voltage restorer (DVR) has been projected. All three FACTS devices including DSTATCOM, DVR and UPQC have been employed to improve power quality and voltage stabilization [27]. Also, in [28], the study investigates the utilization of Unified Power Quality Conditioner (UPQC) to alleviate power quality problems present in the network and harmonics impregnated via non-linear loads. This work supports UPQC through the Photovoltaic (PV) and Battery Energy Storage System (BESS). In [29], the grid system that integrates WE has been found to improve power quality with UPQC. In [30], a method for implementing

an automated transition of a solar photovoltaic system and a unified battery-integrated power quality conditioner (PV-B-UPQC) between stand-alone and grid-connected modes of operation is presented and discussed. The system addresses the issue of integrating power quality improvement with clean energy generation.

Within FACTS techniques based on power electronics, UPQC has a superior performance compared to other techniques, mainly SVC, STATCOM and DVR. UPQC achieves most of the required qualities, comprising voltage enhancement, harmonic alleviation, current enhancement, and complete system power quality improvement [28], [31]. UPQC comprises of shunt and series active power filters (APF) attached through a common DC-link. Shunt APFs recompense reactive power and attenuate load current harmonics, while S-APFs recompense harmonics, sags, swells, and flickers in the source side voltages. The voltage of DC link swing may be controlled through the shunt APF [6]. Particularly, UPQC classifications may do both P-APF and S-APF functionality concurrently. Therefore, UPQC is used in the proposed research to overcome and enhance the power quality owing to the existence of non-linear loads and integration of renewable energy sources into the grid.

In [32], the UPQC provided by photovoltaic modules with boost converter, MPPT P and O, PI, and p-q scheme has been presented. The model was competent to recompense reactive power and decrease load voltage/source current harmonics, but did not address the alleviation of sags and disturbance caused by PV penetration. In [33] PQ alleviation of UPQC-BES on micro-grid provided via PV-Wind hybrid has been employed. The result was that FLC and PI could enhance power quality and diminish distortion in the power of output. The UPQC-wind turbine linked to the UPQC dc-link circuit has been employed in [34]. The proposed arrangement with PI made it possible to recompense over-voltages, voltage disruptions and reactive power both off and on the grid. In [35] the paper deals with the design and performance analysis of a three-phase single stage solar photovoltaic integrated UPQC (PV-UPQC). The proposed system with PI controller combines both the benefits of clean energy generation along with improving power quality. Grid-tied DGs built on wind-PV-UPQC coupled to UPQC DC link have been implemented in [36]. The proposed arrangement with PI has improved PQ issues while providing real power to the grid. In [37], a inclusive study that comprises the sizing and power flow via series and parallel inverters in a distributed generation system (DGs) that integrates the system of hybrid wind photovoltaic with a UPQC is presented. The proposed arrangement with PI has also improved PQ issues while providing real power to the grid. Table 1 presented the comparison of existing methodology with presented work.

The assembly of the standard PI or PID controller, requires an accurate model that operates boundary limits and load disruption affect. In latest years, extensive research has been completed on control circuit strategies for UPQC. The goal is to attain a trustworthy control system and quick response approaches to attain the switch control signals. Currently, artificial intelligence e.g., artificial neural network (ANN) is considered as a latest tool to design control circuits for power quality appliances. Employment of ANN approach in PV-UPQC has been mentioned in [38] to improve power quality. Using ANN delivers fast response compared to traditional PID circuits. This method needs proper training and validation before being implemented in the power system. It takes longer time to gauge the output response of the system, but it provides precise and proper responses. The main contribution of the proposed work is given below:

1. This research work proposes a UPQC with ANN-based controller w.r.t proportional-integral (PI) controller to improve the performance of a DGs that integrates solar PV and wind system.
2. Improved PQ issues such as harmonic attenuation, %THD and power factor (PF) owing to parallel-series power line conditioning abilities. It should be noted that even the PV-wind based system doesn't work because of maintenance work or even during the night, the parallel- series active filtering may continue to function.
3. Inject the power generated by a photovoltaic system and a wind turbine into the grid. In this situation, consumers may or may not be attached to the system. When loads aren't existing, the system functions similar to traditional DGs, in that universal active filtering may be deactivated.
4. To compare performance, the outcomes of the proposed strategy are compared to PI-based control. The performance of two controllers is utilized to determine source current, load voltage, source voltage THD and load current THD according to IEEE-519, in addition to grid and load power factor.

This research paper is structured as follows: Section II presents the explanation of the system of UPQC-ANN-RE, the control of parallel and series NPC inverters and ANN controllers are discussed. Section III discusses the power flow through UPQC-ANN-RE, while Section IV takes an in-depth look at the performance of the UPQC-ANN-RE system using PI and ANN under dynamic and steady-state situations by means of MATLAB/Simulink software. Finally, Section V presents the conclusions.

II. EXPLANATION OF THE UPQC-ANN-RE TOPOLOGY

Figure 1 displays the model proposed in this research. Figure 1 (a) presented the simplified block diagram of the proposed system and Figure 1(b) demonstrated the detailed circuit diagram of the UPQC-ANN-RE System. The RE source based DGs are coupled to the 3P4W distribution system with a frequency of 220 volts (L-L) and 60 Hz via ANN-based UPQC. The assembly is divided into three portions. The first consists of the DGS based on single-stage photovoltaic and wind turbines. The second consists of the NPC series inverter and the passive elements (L filter(L_{sec_abc})) and series coupling transformer. Lastly, the

TABLE 1. Comparison of main features of existing methodology in this literature and this paper.

Ref.	Adopted Methodology	Considered criteria in the formulation of techniques						
		Sources	Intermittency level	THD_{Vs} (%)	THD_{iL}(%)	Static and dynamic response	Accuracy	PF of Utility Grid
[18]	UPQC with PI Controller	PV	Low	Greater	Greater	Slow	Less	Less than Unity
[30]	UPQC-BES using FLC controller	PV and Wind	High	Greater	Greater	Slow	Less	Less than Unity
[33]	PV-UPQC with PI Controller	PV	Low	Greater	Greater	Slow	Less	Less than Unity
[36]	Wind-PV-UPQC with PI Controller	PV and Wind	High	Greater	Greater	Slow	Less	Less than Unity
[37]	PV-wind-UPQC with PI Controller	PV and Wind	High	Greater	Greater	Slow	Less	Less than Unity
This paper	PV-wind-UPQC using ANN Controller	PV and Wind	High	Lower	Lower	Fast	High	Approximately equal to Unity

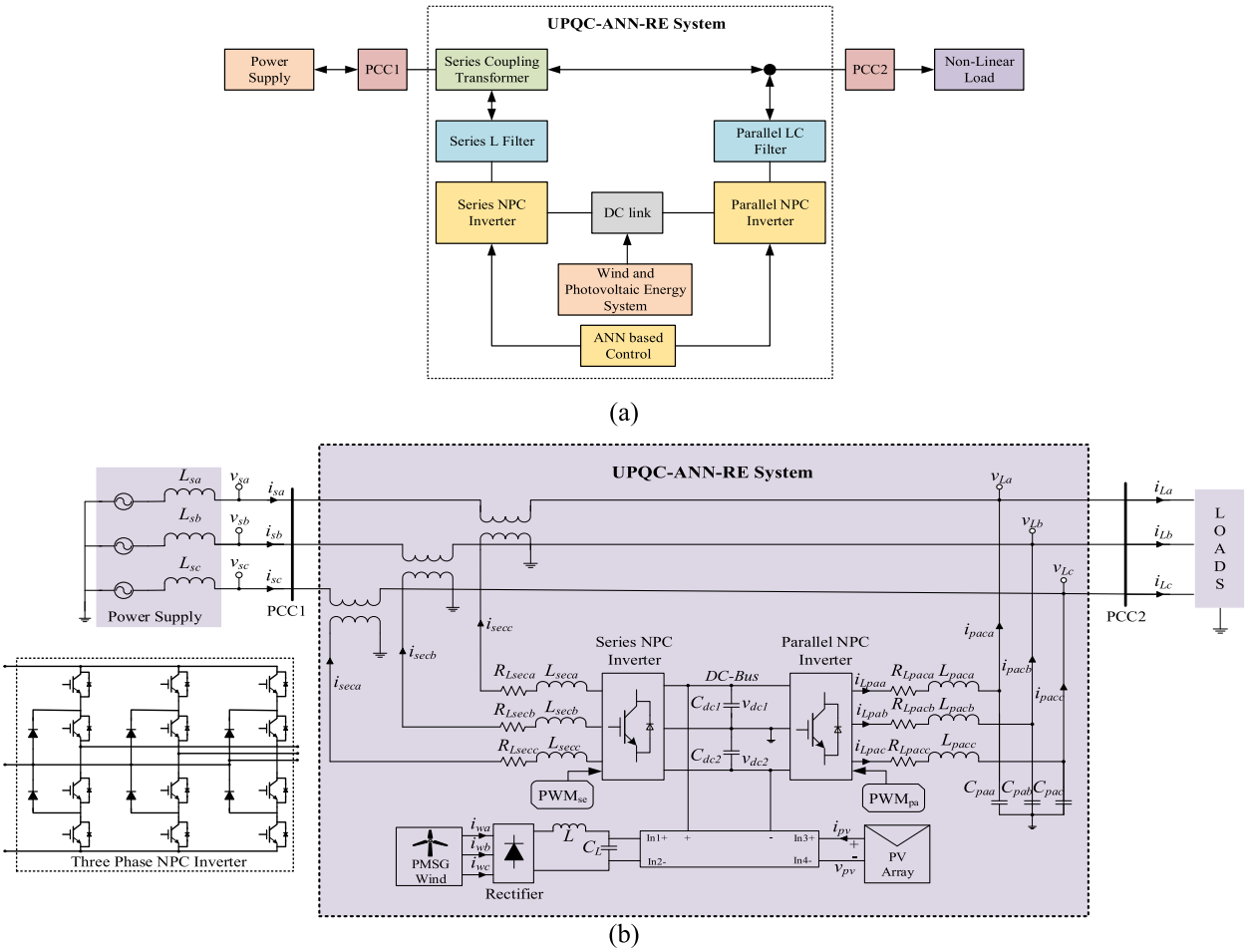

FIGURE 1. (a) Simplified block diagram of the UPQC-ANN-RE system; (b) Circuit diagram of the UPQC-ANN-RE system.

third portion consists of a parallel NPC inverter and filter elements (LC filters (L_{pac_abc} *and* C_{pa_abc})) As may be seen, DGs based on PV- wind and NPC inverters share the identical DC link. Meanwhile the split arrangement of capacitor is utilized, its midpoint of the DC bus must be attached to the neutral conductor which makes local 3P4W system.

The DGs deprived of storage consists of a photovoltaic network composed of a single string of twenty photovoltaic modules connected in series and a permanent magnet synchronous generator (PMSG) wind turbine that have the fixed voltage and variable speed which produces electricity and is linked to the dc link of UPQC via an AC/DC bridge rectifier.

The MPPT algorithm makes a vital role to producing maximum power under different weather conditions. Therefore, the system of UPQC-ANN-RE is designed to function with the reference of DC bus voltage v^*_{dc} determined via the MPPT process [39]. So, the maximum magnitude of the voltage of DC bus ($v^*_{dc\_max}$) is about 600 V, which allows the system to operate under standard test conditions (STC) in the MPP. In contrast, the least working voltage of the system ($v^*_{dc\_min}$) is fixed at 460 V, i.e. when this voltage is touched, the system operates outside the MPP.

A. CONTROL OF UPQC-ANN-RE SYSTEM

The compensation scheme utilized in the system of UPQC-ANN-RE is recognized as the dual compensation approach and in detail is discussed in [40], [41], and [42], there the advantages over traditional compensation schemes [43] utilized to control utmost UPQCs described in the literatures are discussed. With the dual compensation approach, the NPC series inverter should be controlled like a sinusoidal current source. In contrast, the NPC parallel inverter should be controlled like a sinusoidal voltage source.

1) NPC SERIES INVERTER CONTROL

In it, the sine waves and symmetrical currents of the NPC series inverter are controlled to remain in-phase with voltages of grid. This recompenses for load imbalances and reactive power and suppresses harmonic currents, ensuring effective PF correction. Additionally, the path of high impedance formed via the sine current-controlled NPC series inverter pushes harmonic currents to flow from the load over the NPC parallel inverter.

The procedures utilized to produce the grid current (NPC series inverters) and DC bus voltages (MPPT P&O) references are displayed in Figure 2. Primary, the load currents are evaluated and converted from the *abc* axis to *dq* axis. thus the current i_{Ld} n be obtained directly as:

$$i_{Ld} = \sqrt{2/3}\left[cos\theta - \frac{1}{2}cos\theta + \frac{\sqrt{3}}{2}sin\theta - \frac{1}{2}cos\theta + \frac{\sqrt{3}}{2}sin\theta\right] \times \begin{bmatrix} i_{La} \\ i_{Lb} \\ i_{Lc} \end{bmatrix} \quad (1)$$

The current i_{Ld}s formed by the load current harmonic and real components, here $cos\theta$ and $sin\theta$ are the coordinates of the rotating unit vector. A PLL [44] is using to gauge the phase angle of the voltage of source $\theta = \theta_{pll}$.

The mean of $i_{Ld}(i_{Ld_{dc}})$ is attained with a low pass filter (LPF) such that $i_{Ld_{dc}}$are real components of the *abc* load currents. Finally, the reference of NPC series inverter input current on d-axis is given by:

$$i^*_{secd} = i_{Ld_{dc}} + i_{dc} - i_{ff} \quad (2)$$

Here i_{dc} is the ANN controller DC link voltage output signal and i_{ff} is feed forward current. The i_{dc} illustrates the amount of real power handled via NPC series inverter to make sure the stability of the UPQC power and thus control the voltage of DC bus. That is to say, i_{dc} modified the magnitude of i^*_{secd} to regulate the power flow via the system of UPQC-ANN-RE and performs energy stability. Along with i_{dc} the quantityi_{ff} speeds up the balance of energy. Since currents that are balanced and sine-waves, are expected in the power grid, together the zero-sequence component (i^*_{sec0}) and the quadrature current (i^*_{secq}) are set to be zero.

2) NPC PARALLEL INVERTER CONTROL

The core purpose of the NPC parallel inverter is to supply voltages that are regulated, symmetrical and sinusoidal, to the load. The voltages of output are all the time controlled to remain in-phase with the positive sequence constituent of the mains voltages in it. In that situation, merely real power may be sent/ drawn to/from the grid through the NPC series inverter to sustain the system power stability while the input and output voltage magnitudes vary from one another. Additionally, the path of less impedance formed via the sine wave voltage controlled NPC parallel inverter permits harmonic currents of load to flow over the NPC parallel inverter. That one may be pointed out that PQ happenings occur via series coupling transformers resulting in indirect voltage recompense/suppression.

The procedures utilized to produce the output voltage references (NPC parallel inverters) are displayed in Figure 3. The references of input voltage of NPC parallel inverter are fixed to $V^*_{L\_abc}$ and V^*_{Ld} in *abc* and d-axis, respectively, as displayed in Figure 3. As voltages that are symmetrical and sine wave, are provided to the load, the zero-sequence component V^*_{L0} and the quadrature voltage V^*_{Lq} are fixed to be zero [18], [36].

3) ARTIFICIAL NEURAL NETWORK

ANN is one of the AI approaches that perceives a very suitable application for the control of power electronic systems. A latest study shows that ANN-based controllers offer quicker dynamic reaction and enhanced the constancy of converter structures over a vast range of operating situations. The advantages of ANN comprise learnability, error tolerance, adaptability, generalizability, contextual data processing, less power utilization, traceability, robustness and fast convergence [45], [46]. The main ANN design consists of three layers and is presented in Figure 4.

1. Input Layer: It saves the data of input as well as the inputs that will be given to the model are providing by this layer.
2. Hidden layer: The input delivered via the input layer is handled in hidden layer according to the weight of

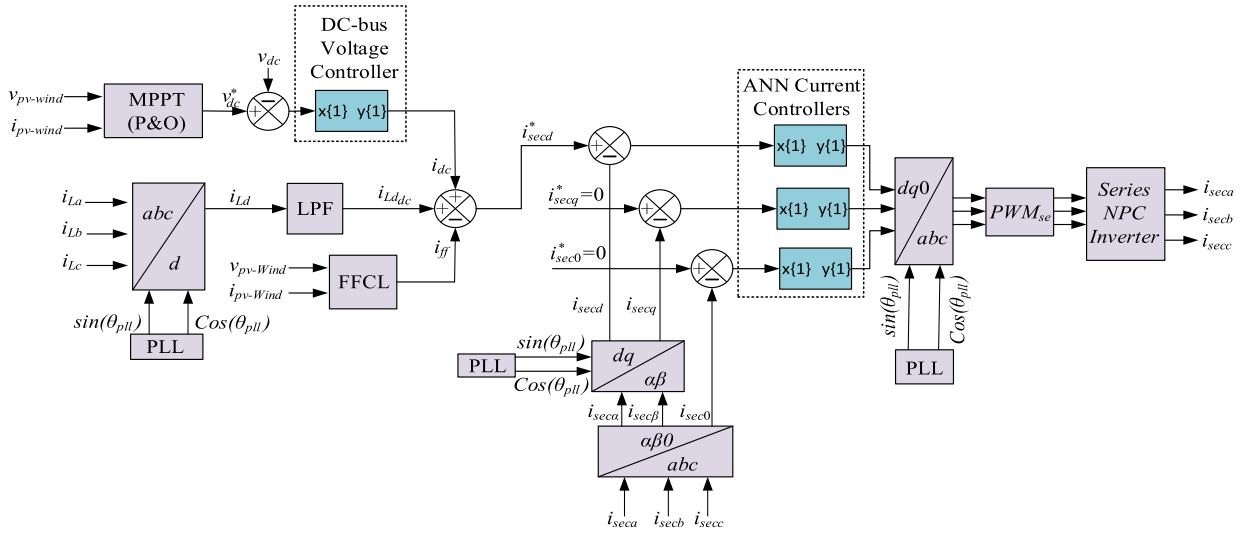

FIGURE 2. Control strategy of series converter.

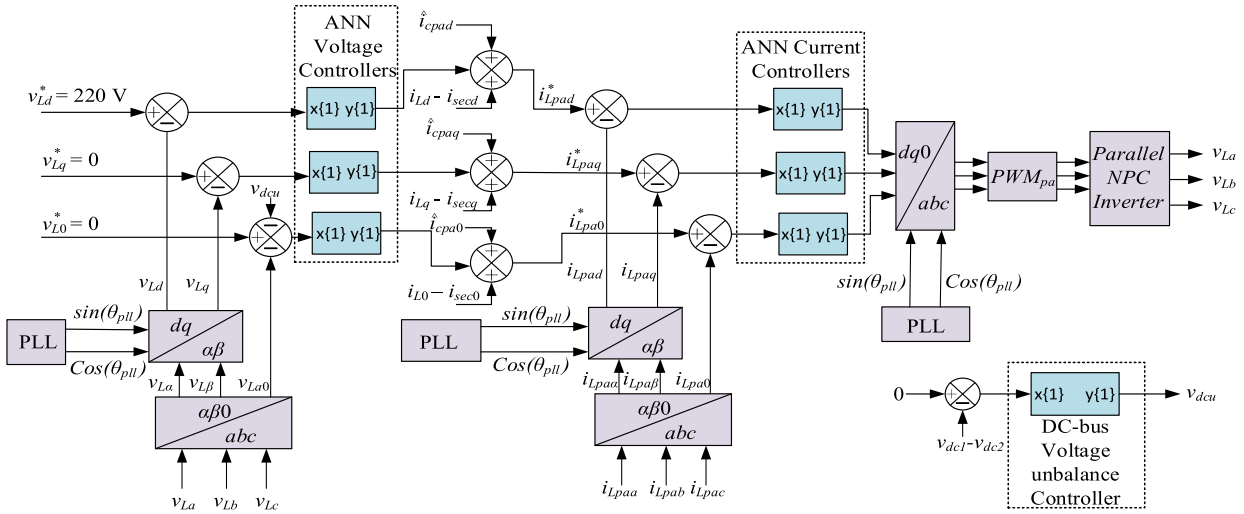

FIGURE 3. Control strategy of parallel converter.

the connection among the layers, any biases and the functions of activation.

3. Output layer: the consequences of the calculations are saved.

An artificial neural network algorithm characterized by the following steps:

Step 1: Process each signal input to the node of the neural network input layer and determine its weight W;

Step 2: Repeat the succeeding process until convergence: (1) For $k = 1$ to N;

Calculate the values of O_{ik}, net_{jk} and;

(2) Calculate δ_{jk} for the same node $j \in M$;

Step 3: Correct the weights;

Step 4: Given the neural network node attribute sample set M, the neural network node attribute set $F = \{F_1, F_2 \ldots F_i \ldots F_t\}$. The number of branches N and the branch stopping criterion, the specific steps of the procedure are as follows:

(1) Judge whether the current node meets the stopping condition according to the branch stopping criterion. If so, return the empty tree and input the data A; Otherwise, go to Step (2).

(2) According to the neural network node attribute sample set M, for t attributes in the neural network node attribute set F. When F_i is used to judge the attribute, the corresponding impurity change is the Gini index change $F_i(M)$.

(3) Select the attribute with the largest change of Gini index value $F_i(M)$, and take this attribute as the split genus of this branch F_m;

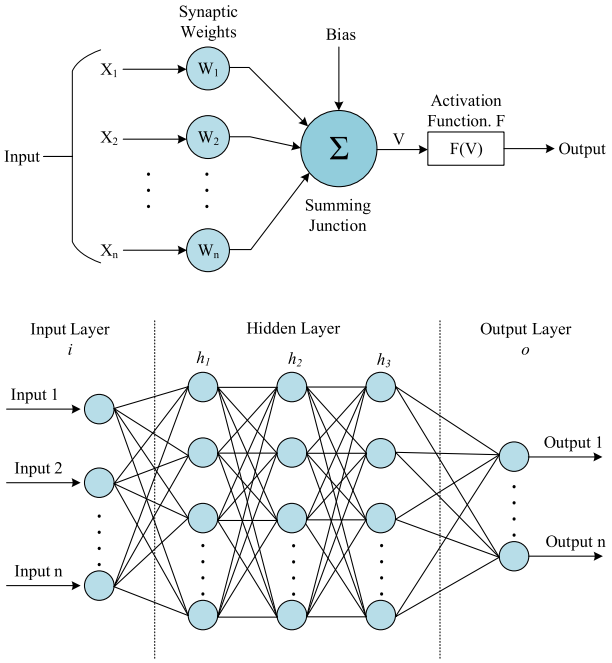

FIGURE 4. Basic ANN structure.

(4) (4) According to the splitting attribute F_m, the neural network node attribute sample set is divided into N subsets.
(5) Perform steps (1) ∼ (4) on N subsets respectively, and the new input is subset N_j and attribute set F, so as to obtain the relative score classifier T_j (possibly empty tree) for clade N_j;
(6) Pruning the established decision tree to obtain a series of nested subtrees;
(7) V-fold cross validation was used to select the optimal subtree;
(8) The optimal decision tree is selected to determine the conditions of the new test samples, and the corresponding classification results are output.

Step 5: After determining the output classification results in Step 4 each time, the classification results shall be corrected and learned to make errors. The signal is minimal until the current node meets the stop condition, after which the diagnostic data is output.

2. According to point 1, an artificial neural network algorithm is characterized as follows: in step 1, if the input

If there is more than one signal, there are x input signals: $P_1, P_2, P_3 \ldots P_x$, the input signal is processed first, and the weight value of each input signal is determined: $\omega_3, \omega_4 \ldots, \omega_x$, and then calculate the weighted sum through the formula:$W = W_1, P_1 + W_2, P_2 + \ldots + w_x, p_x + b$ where b is the bias index.

3. According to the artificial neural network algorithm mentioned in point 2, its characteristics are as follows: the artificial neural network may also have one or more hidden layer nodes; For the input signal, it should first propagate forward to the hidden layer node, and then after the conversion of the excitation function

The output signal of hidden layer node is propagated to the output node, and finally the output result is given.

4. According to the artificial neural network algorithm mentioned in point 3, its characteristics lie in: the excitation function of the node: $f(x) = \delta(x)$

5. According to the artificial neural network algorithm mentioned in point 4, its characteristics are as follows: the excitation function of the node is the body relation is:

$$f(x) = \frac{1}{1 + e^{-x/Q}} \tag{3}$$

where, Q is the Sigmoid parameter in the form of adjustment excitation function.

6. According to an artificial neural network algorithm mentioned in point 1, its characteristics are as follows: the error correction learning process is composed of forward propagation and back propagation; In the forward propagation process, the input information is processed layer by layer from the input layer through the hidden layer and transmitted to the output layer. The states of neurons in each layer only affect the states of neurons in the next layer; If the output layer does not get the desired output, it will turn to back propagation and return the error signal along the original connection channel. By modifying the weights of neurons in each layer, the error signal will be minimized.

7. According to an artificial neural network algorithm mentioned in point 6, its characteristics are as follows: the calculation formula of the error correction learning process of the algorithm is: suppose an arbitrary network with N nodes, and the activation function of each node is purelin type; For simplicity, specify that the network has only one output Y, the output of any node I is O_i, and set N samples (x_k, y_k) $(k = 1, 2, \cdots N)$.

For some input x_k, the network output is y_k, the output of node I is O_{ik}, and the input of node j is:

$$net_{jk} = \sum_i W_{ij} O_{ik} \tag{4}$$

And the error function is defined as:

$$E = \frac{1}{2} \sum_{k=1}^{N} \left(y_k - \hat{y}_k\right)^2 \tag{5}$$

where is $\hat{y}_k$ the actual network output, defined an $E_k = \left(y_k - \hat{y}_k\right)^2$, $\delta_{jk} = \frac{\partial E_k}{\partial net_{jk}}$, and $0_{jk} = f\left(net_{jk}\right)$, then:

$$\frac{\partial E_k}{\partial W_{ij}} = \frac{\partial E_k}{\partial net_{jk}} \frac{\partial net_{jk}}{\partial W_{ij}} = \frac{\partial E_k}{\partial net_{jk}} O_{ik} = \delta_{jk} O_{ik} \tag{6}$$

$$\delta_{jk} = \frac{\partial E_k}{\partial \hat{y}_k} \frac{\partial \hat{y}_k}{\partial net_{jk}} = -\left(y_k - \hat{y}_k\right) f'\left(net_{jk}\right) \tag{7}$$

If j is not an output node, yes?

$$\delta_{jk} = \frac{\partial E_k}{\partial net_{jk}} = \frac{\partial E_k}{\partial O_{jk}} \frac{\partial O_{jk}}{\partial net_{jk}} = \frac{\partial E_k}{\partial O_{jk}} f'\left(net_{jk}\right)$$

$$\frac{\partial E_k}{\partial O_{jk}} = \sum_m \frac{\partial E_k}{\partial \text{net}_{mk}} \frac{\partial \text{net}_{mk}}{\partial O_{jk}} = \sum_m \frac{\partial E_k}{\partial \text{net}_{mk}} \frac{\partial}{\partial O_{jk}} \sum_i W_{mi} O_{ik} = \sum_m \frac{\partial E_k}{\partial \text{net}_{mk}} \sum_i W_{mj} = \sum_m \delta_{mk} W_{mj} \tag{8}$$

Hence

$$\begin{cases} \delta_{jk} = f'\left(\text{net}_{jk}\right) \sum_m \delta_{mk} W_{mj} \\ \dfrac{\partial E_k}{\partial W_{ij}} = \delta_{mk} O_{ik} \end{cases} \tag{9}$$

8. An encapsulation document characterized in that it includes an artificial neural network algorithm of any of the points 1-7. By encapsulating the algorithm into a file, the system calls the encapsulated text when a set of data devices is entered to realize the data diagnosis output.

Levenberg-Marquardt backpropagation (LMBP) [47], [48], [49] is one of the ANN training methods that achieves quicker convergence, especially when the function is the mean square fault. Although that one is a multi-layered Feed-Forward system alike the well-known error backpropagation, it is still different as it uses the resultant derivatives to update the weights. Inputs from the layer of input are sent to the hidden layers using weights assigned separately to every link. The overall durability of a node's input is checked by the functions of activation, and based upon the outcomes, the nodes of hidden layer activate their inputs to the layers of output. The outcome to the targets are compared via output, and still there is an error, then the weights of link are altered so that for the succeeding iteration of inputs, the outputs are as required. This procedure lasts till convergence. In this research, an ANN-based UPQC is constructed to enhance the PQ of a hybrid green power system with the following parameters: ANN: number of hidden layers: 30, number of epochs: 5000, number of inputs: 1 and outputs: 1 of error controllers (PI or P). Table 2 presents the network parameters that are used while training the system.

TABLE 2. Parameters of neural network used in training.

Structure of ANN model	Training algorithm	Activation function	Train Mean Squared Error (MSE)	Correlation coefficient R	
				Training	Testing
1:30:1	trainlm	purelin	6.03e-07	1	1

III. ACTIVE/REAL POWER FLOW VIA THE UPQC-ANN-RE SYSTEM

Table 3 illustrates the four possible operating conditions that may be deliberated. In the proposed model, the way of real power flow over the NPC parallel (P_{pac}) and NPC series (P_{sec}) inverter could vary depend on the succeeding situations:

TABLE 3. Conditions implemented to govern an active/real power flow by UPQC-ANN-RE system.

Operating conditions		RMS voltages	PV and wind power	Load power
a	1	$V_s > V_L$	$P_{pv-wind} = 0$	$P_L \neq 0$
	2	$V_s < V_L$		
b	1	$V_s > V_L$	$P_{pv-wind} > 0$	$P_L = 0$
	2	$V_s < V_L$		
c	1	$V_s > V_L$	$P_{pv-wind} < P_L$	$P_L > 0$
	2	$V_s < V_L$		
d	1	$V_s > V_L$	$P_{pv-wind} > P_L$	$P_L > 0$
	2	$V_s < V_L$		

1. Quantity of real power produced via PV system and wind turbine ($P_{pv-wind}$).
2. Quantity of active power spent through loads (P_L).
3. The difference in the effective values of source voltage (V_s) and load voltage (V_L).

Considering all the conditions presented in Table 3 and Figure 5, at $V_s = V_L$, the active power flowing over the series converter (P_{sec}) is 0 W. In that instance, the system is deliberated theoretically ideal.

Figure 5(a) demonstrates the energy flow when PV and wind turbines are not functioning. In that instance, the real powers required via the loads flow to series inverter from the grid and to load from the parallel inverter. Figure 5(b) demonstrates the real power flow while the power required at the load is 0 W. In this state, all power flows to the grid from the DC bus. Most of power is still handled via the parallel converter. Figure 5(c) demonstrates the real power flow while the power produced via photovoltaic array and the wind turbine is insufficient to feed the loads. In this instance, the extra energy required via these loads must flow to the load from the utility grid over the parallel and series converter. Lastly, Figure 5(d) demonstrates when the energy produced via the PV and wind turbine is greater ac compare to the total energy spent via the loads. In that state, excess flow of energy to utility grid from DC bus and the rest is referred to the load.

IV. RESULTS AND ANALYSIS

The UPQC-ANN-RE system performance analysis is analyzed by run the system in the software of MATLAB/Simulink. The system simulations are implemented depend upon the schematic presented in Figure 1. The 3-level NPC inverters constitute the parallel and series PWM converters. Table 4 summarizes the core parameters of simulation. The nonlinear load comprising of a 3-phase diode bridge rectifier with R load is utilized as load. The step size of the solver used for the simulation is 5.0505e-6s.

To analyzing the proposed model, the four operating conditions (OPC) are used. For OPC 1, which arises at

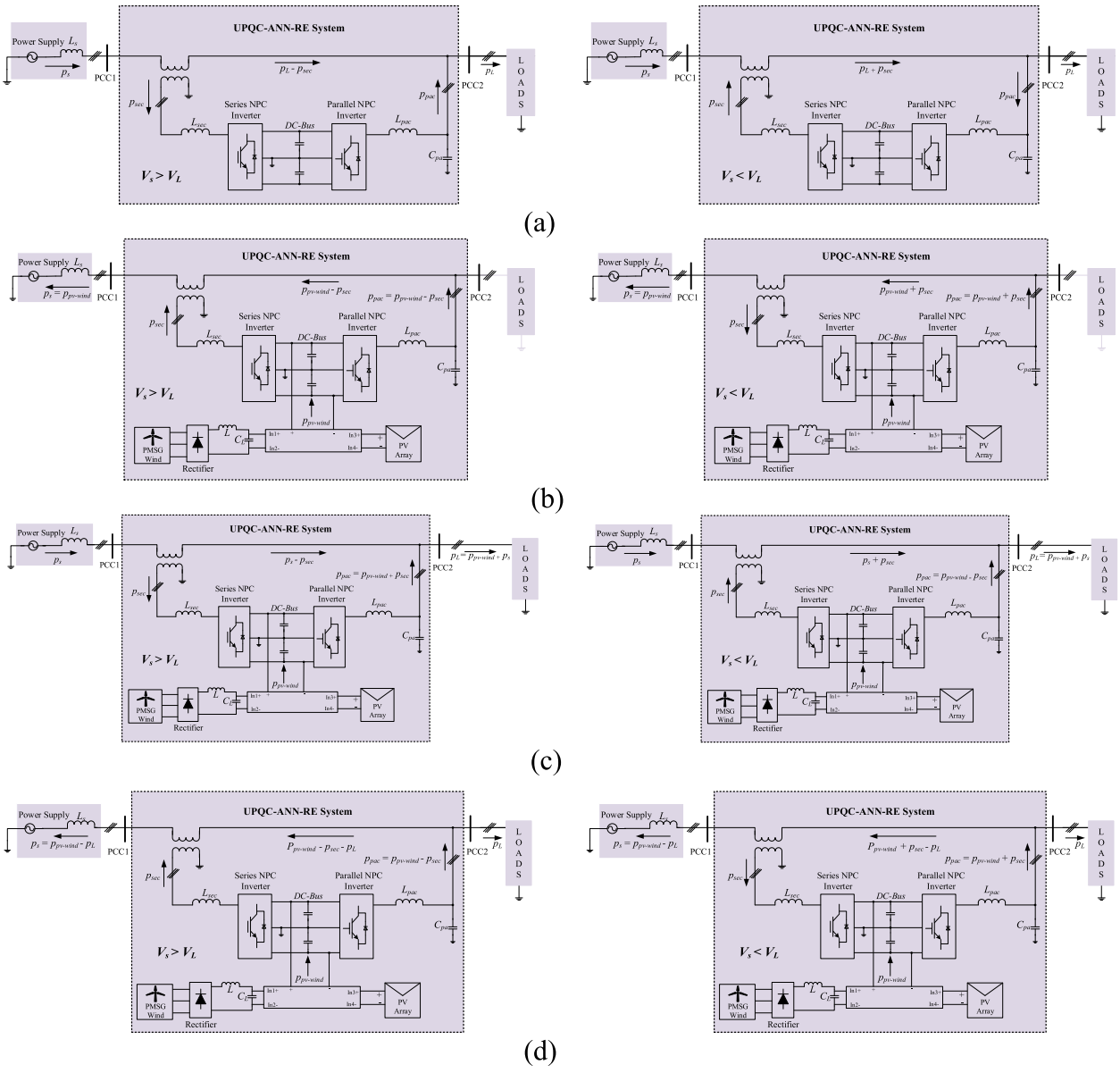

FIGURE 5. Active power flow by UPQC-ANN-RE system (a) $P_{pv-wind} = 0$ W; (b) $P_L = 0W$; (c) $P_{pv-wind} < P_L$; (d) $P_{pv-wind} > P_L$.

night-time (deprived of solar radiation), the model functions only like a UPQC-ANN-RE. Thus, $P_{pv-wind} = 0$W. In OPC 2, the UPQC-ANN-RE system functions without the load and simply inserts active/real power in the utility grid. OPC 3 occurs when there is solar insolation and at the same time energy is needed by the load linked with the system of UPQC-ANN-RE so that $P_{pv-wind} < P_L$. Lastly, like OPC 3, OPC 4 arises when$P_{pv-wind} > P_L$. Each OPC of UPQC utilizing a PI and ANN controller, so the entire number of situations is 8.

Utilizing Matlab/Simulink, the system is simulate under the preferred situations to attain the waveforms of grid voltages (V_s), load voltages (V_L), parallel NPC inverter currents (i_{pac}), grid currents (i_s), load currents (i_L), PV and Wind turbine Current ($i_{pv-wind}$), PV and Wind turbine power $P_{pv-wind}$ and DC link voltages (V_{dc}). The procedure of the proposed system is well described in Figure 6.

Then, value of THD of the grid current and voltage, load current and voltage in every phase and the average value of THD are attained according to the curves. The average grid current and voltage, load current and voltage results for 3P4W system utilizing a UPQC-ANN-RE system powered by PV-wind RE sources, are presented in Table 5. Afterward THD in every phase and the average of THD are displayed in the Table 6. In addition, the average power factor of the grid and the load are also shown in Table 7.

Table 5 illustrates the UPQC-ANN-RE system utilizing PI and ANN, conditions 1 generate a mean load voltage of around 140 V (L-N) and conditions 2 to 4 generates a mean load voltage of about 128 V (L-N). From the table we can also

TABLE 4. Parameters assumed in the simulation.

Three phase Grid	
Nominal utility voltages (RMS)	V_s =127.27 V
Utility grid frequency	f_s = 60 Hz
Leakage inductance of series coupling transformers	L_T = 0.3 mH
Resistances of series coupling transformers	R_T = 0.28 Ω
Turn ratio of the series transformer	n_T = 1:1
Inductive filters (series NPC inverter)	L_{sec} = 1.75 mH
Internal resistances of the series NPC inverter inductors	R_{sec} = 0.2 Ω
Inductive Filters (parallel NPC inverter)	L_{pac} = 1.73 mH
Internal resistances of the parallel NPC inverter inductors	R_{pac} = 0.2 Ω
Capacitive filters (parallel NPC inverter)	C_{pac} = 60 μF
dc-bus equivalent capacitance	C_{dc} = 4700 μF
dc-bus voltage (MPP in STC)	V_{dc} = 616 V
Minimum dc-bus voltage	v^*_{dc} = 460 V
PWM gain	C_{pwm} = 0.0002
Photovoltaic	
Active Power	2.0 KW
Temperature	25°C
Irradiance	600 W/m^2
PMSG wind turbine	
Active Power	1.5 KW
Speed of Wind	8 m/s
Pitch angle of Blade	0 degree
Non-Linear Load	
Three-phase diode bridge rectifier with resistive load	R = 40 Ω

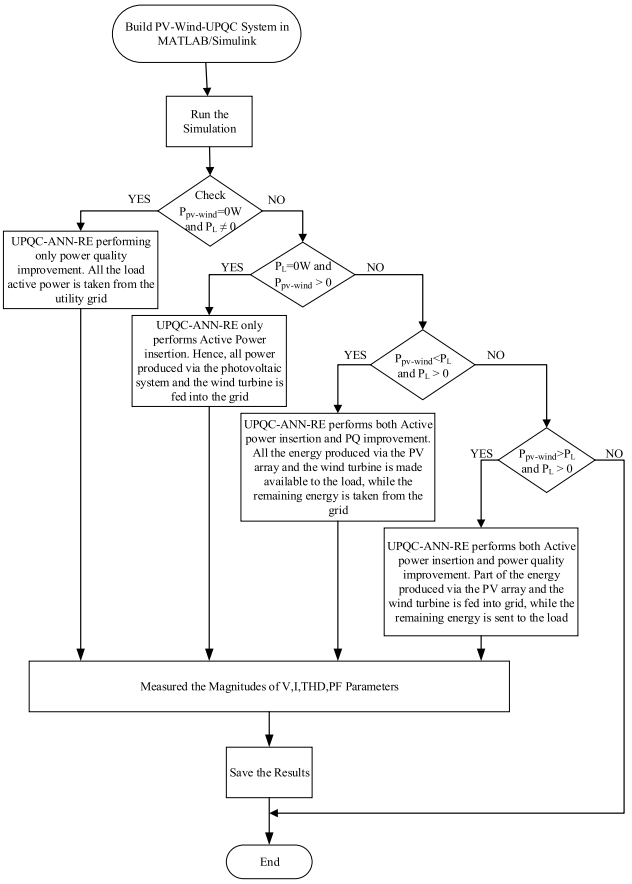

FIGURE 6. The simulation flowchart.

see that in both cases the value of an average grid current is approximately the same.

Table 6 demonstrates that the average load voltage THD of the system of UPQC-ANN-RE for conditions 1 to 4 with PI is in the limits of the IEEE-519 standard.

The uppermost and lowermost average THD of load voltage are attained in conditions 1 and 2 at 3.1% and 2.0%, respectively. The PI can also attenuate the average THD grid voltage and current and load current under all conditions. The uppermost and lowermost average harmonic distortion of the grid current is reached in conditions 3 and 4 with 5.3% and 1.5% respectively. That is also noticed that the average THD of the load current is almost 28%, thus meeting the requirement of the IEEE519 standard. Table 6 also demonstrates that the average load voltage THD of the UPQC-ANN-RE system with ANN for conditions 1 to 4 complies with the limit values of the IEEE 519 standard. The uppermost and lowermost average load voltage THDs are attained in conditions 1 and 2 are 2.9% and 1.9%, respectively. The ANN technique is too

TABLE 5. RMS voltage and current of UPQC-ANN-RE system.

Operating conditions	Grid Voltages V_s (V)				Load Voltages V_L (V)				Grid Currents I_s (A)				Load Currents I_L A)			
	Ph "a"	Ph "b"	Ph "c"	Avg	Ph "a"	Ph "b"	Ph "c"	Avg	Ph "a"	Ph "b"	Ph "c"	Avg	Ph "a"	Ph "b"	Ph "c"	Avg
PI Controller																
OPC1	127.6	127.6	127.6	127.6	140.3	139.9	140	140	7.98	7.98	7.97	7.98	6.68	6.70	6.69	6.69
OPC2	127.2	127.2	127.2	127.2	129.8	129.9	129.9	129.9	8.04	8.02	8.04	8.03	---	---	---	---
OPC3	127	127	127	127	126	126	126	126	4.34	4.35	4.36	4.35	7.18	7.19	7.18	7.18
OPC4	127.1	127.1	127.1	127.1	128.2	128.2	128.1	128.2	2.85	2.84	2.84	2.84	6.03	6.02	6.01	6.02
ANN Controller																
OPC1	127.6	127.6	127.6	127.6	140	140.1	140.1	140.1	7.99	7.98	7.98	7.98	6.69	6.71	6.70	6.70
OPC2	127.2	127.2	127.2	127.2	129.8	129.9	129.9	129.9	8.02	8.03	8.03	8.03	---	---	---	---
OPC3	127	127	127	127	126	126	126	126	4.6	4.6	4.6	4.6	7.19	7.17	7.19	7.19
OPC4	127.1	127.1	127.1	127.1	128.3	128.3	128.3	128.3	3.1	3.1	3.1	3.1	6.03	6.04	6.01	6.03

TABLE 6. Harmonics of UPQC-ANN-RE system.

Operating conditions	Grid Voltage THD (%)				Load Voltage THD (%)				Grid Current THD (%)				Load Current THD (%)			
	Ph "a"	Ph "b"	Ph "c"	Avg	Ph "a"	Ph "b"	Ph "c"	Avg	Ph "a"	Ph "b"	Ph "c"	Avg	Ph "a"	Ph "b"	Ph "c"	Avg
PI Controller																
OPC1	1.0	1.0	1.1	1.0	3.1	3.1	3.2	3.1	2.0	1.9	2.2	2.0	29	28	29	28.7
OPC2	1.7	1.5	1.6	1.6	2.4	1.9	1.6	2.0	2.5	2.6	2.4	2.5	---	---	---	---
OPC3	1.7	1.8	1.7	1.7	2.5	2.2	1.7	2.1	5.5	5.5	4.8	5.3	29	29	28	28.7
OPC4	1.5	1.4	1.5	1.5	2.6	2.2	1.7	2.2	1.5	1.4	1.5	1.5	28	28	27	27.7
ANN Controller																
OPC1	0.8	0.7	0.7	0.7	2.8	2.8	3.0	2.9	1.9	1.9	2.0	1.9	28	28	28	28
OPC2	1.5	1.5	1.7	1.6	2.3	1.7	1.6	1.9	2.4	2.4	2.4	2.4	---	---	---	---
OPC3	1.5	1.6	1.6	1.6	2.4	2.1	1.5	2.0	5.4	5.4	4.5	5.1	27	27	28	27.3
OPC4	1.5	1.4	1.3	1.4	2.5	2.2	1.5	2.1	1.3	1.4	1.3	1.3	27	27	27	27

TABLE 7. Power factor of UPQC-ANN-RE system.

Operating conditions	Grid PF				Load PF			
	Ph "a"	Ph "b"	Ph "c"	Avg	Ph "a"	Ph "b"	Ph "c"	Avg
PI Controller								
OPC1	0.98	0.98	0.98	0.98	0.96	0.96	0.95	0.96
OPC2	-0.99	-0.98	-0.99	-0.99	---	---	---	---
OPC3	0.98	0.98	0.98	0.99	0.96	0.96	0.96	0.96
OPC4	-0.98	-0.98	-0.98	-0.98	0.96	0.95	0.96	0.96
ANN Controller								
OPC1	0.99	0.98	0.99	0.99	0.96	0.96	0.96	0.96
OPC2	-0.99	-0.99	-0.99	-0.99	---	---	---	---
OPC3	0.99	0.98	0.98	0.98	0.96	0.96	0.96	0.96
OPC4	-0.98	-0.99	-0.99	-0.99	0.96	0.96	0.96	0.96

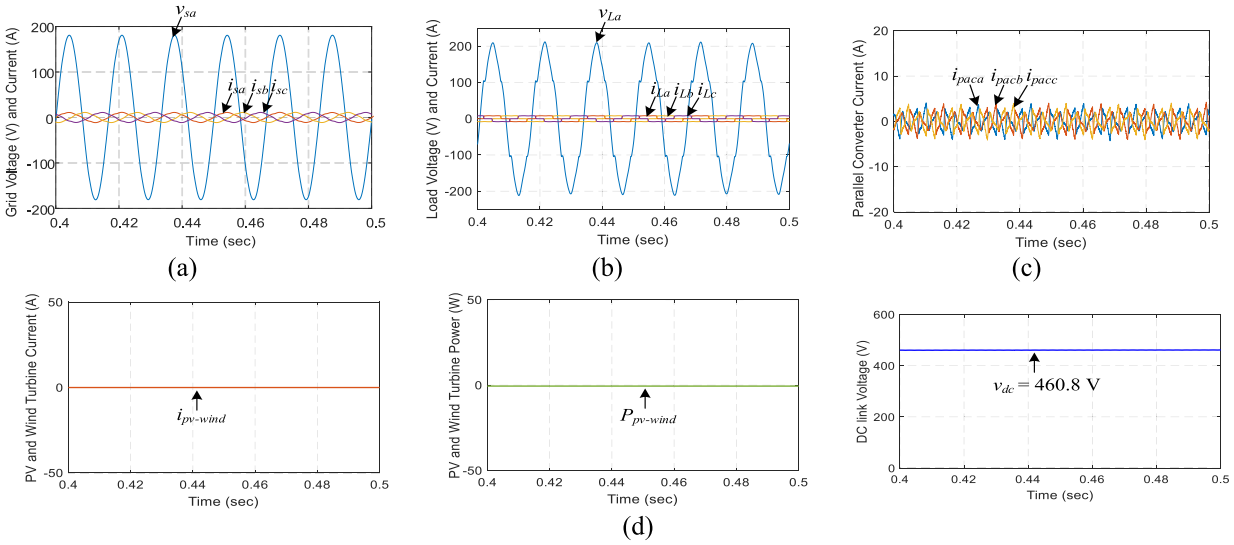

FIGURE 7. OPC 1: UPQC-ANN-RE only performs active/real power-line conditioning with $P_{pv-wind} = 0$ W and $V_s < V_L$ (a) Voltage and current of Grid; (b) Voltage and current of load; (c) currents of Parallel NPC Inverter; (d) PV array and Wind turbine current, Power and DC link voltages.

capable to diminish an average THD of grid current and voltage and load current under all situations. The uppermost and lowermost average grid current THDs are obtained in conditions 3 and 4 as 5.1% and 1.3%, respectively. That is also noticed that the THD of load current is almost 27%, so it meets the requirement of IEEE519 standard. In general, the ANN implementation in the UPQC-ANN-RE system is competent to attain the average THD of load voltage/grid current slightly better as compared to PI.

Table 7 shows an average grid and load related power factor (PF) of the UPQC-ANN-RE system for conditions 1 to 4 using PI and ANN controllers. As can be seen, effective PF corrections were obtained in both cases, but the ANN-based UPQC system gives slightly improved results.

Figure 7 demonstrates the steady state performance analysis waveforms of the UPQC-ANN-RE system operating as UPQC (OPC 1), i.e., with $P_{pv-wind} = 0$W, while $V_s < V_L$ As can be seen, the parallel inverter provided regulated,

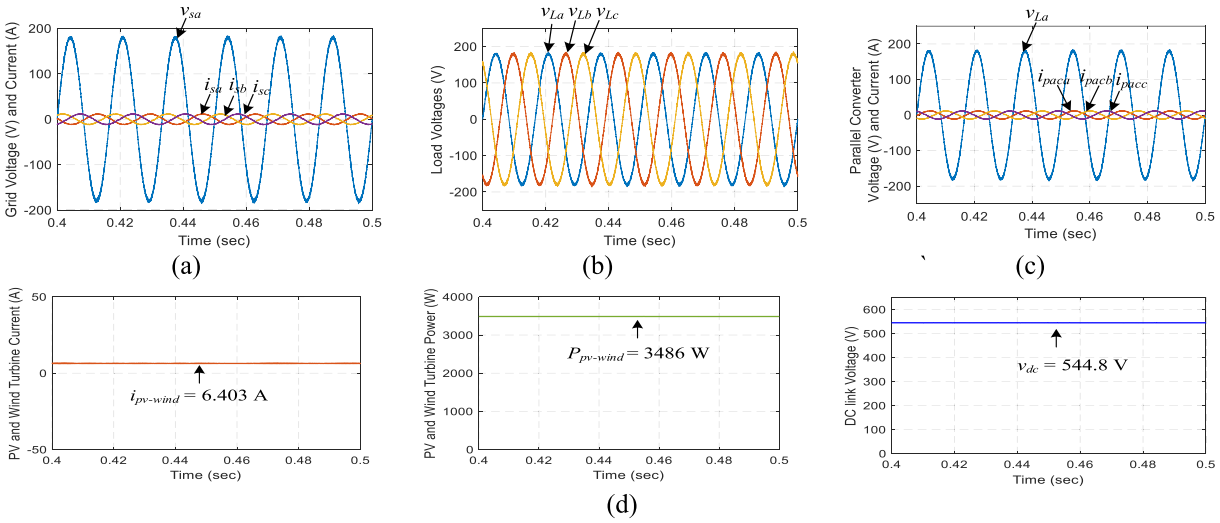

FIGURE 8. OPC 2: UPQC-ANN-RE performs simply active power insertion in the utility grid with $P_L = 0$ W and $P_{pv-wind} = 3500$ W: (a) Voltage and current of Grid; (b) Voltage of load; (c) Voltage of Load and currents of Parallel NPC Inverter; (d) PV array and Wind turbine current, Power and DC link voltages.

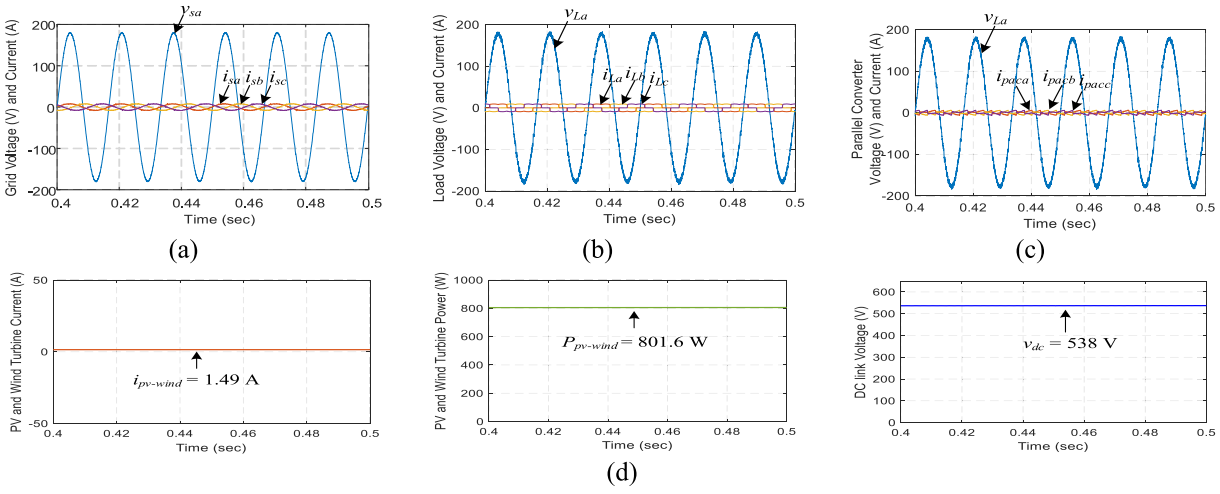

FIGURE 9. OPC 3: UPQC-ANN-RE performs active power insertion along with active filtering with $P_{pv-wind} < P_L$: (a) Voltage and current of Grid; (b) Voltage and current of load; (c) Voltage of Load and Parallel NPC Inverter currents; (d) PV array and Wind turbine current, Power and DC link voltages.

symmetrical and sine wave voltages to the load. It is also noted that the current of grid are in phase and sinusoidal with their corresponding voltages, that is to say that rather than the grid the harmonic constituents of the load current cross the parallel inverter.

Figures 8 through 10 show the steady-state performance analysis waveforms of the UPQC-ANN-RE system inserting active power into the grid. In Figure 8, $P_{pv-wind} \cong 3500$ W, load is detached and merely the real power is inserted in the utility grid (OPC 2). As may be observed, the current of grid are in opposition phase and sinusoidal at the corresponding voltage of supply. In Figure 9, $P_{pv-wind}$ is less than P_L (OPC 3). In this state, the system draws power from the utility grid due to the power of the photovoltaic generator and the wind turbine is lower as compare to the active power needed by the load. Therefore, the UPQC-ANN-RE system, together with the grid, provides the load. OPC 4 arises when $P_{pv-wind}$ is greater as compare to the load real power P_L, as presented in Figure 10. In this situation, the load is supplied via the UPQC-ANN-RE system and the excess of the real power produced is directed toward the grid. In addition, the NPC series inverter produces sine wave currents in phase opposite to the corresponding grid voltages. As can be seen, the UPQC-ANN-RE system does active/real power-line conditioning both in OPC 3 and OPC 4.

From the steady state outcomes illustrated in Figures 7-10 and Tables 5, 6 and 7, it may be proved that the system is capable of operating under different operating conditions and supplying the loads with regulated, sinusoidal and symmetrical voltages. Additionally, the system is able to efficiently

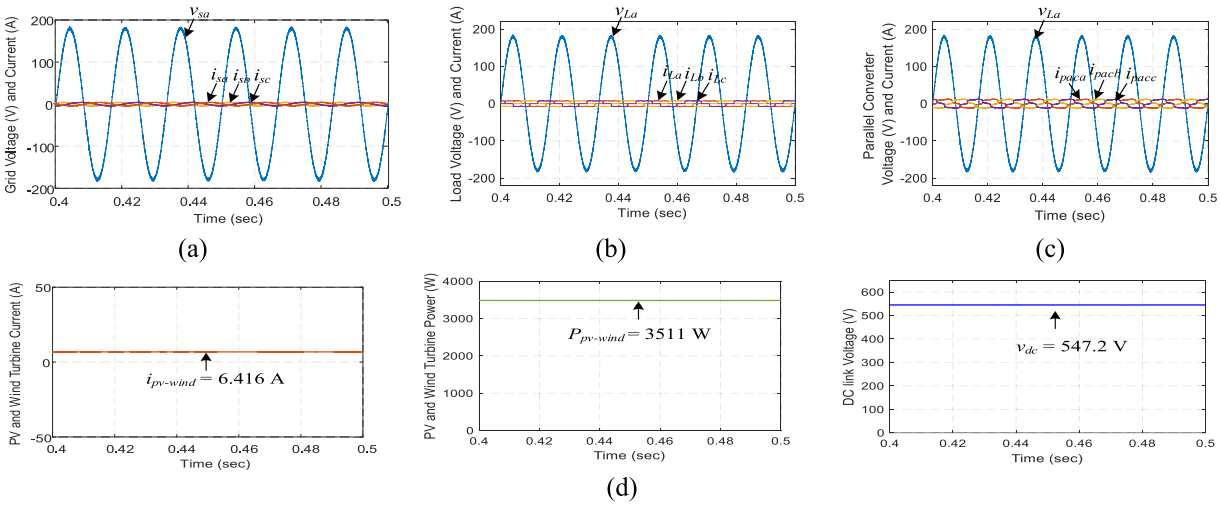

FIGURE 10. OPC 4: UPQC-ANN-RE performs active power insertion along with active filtering with $P_{pv-wind} > P_L$: (a) Voltage and current of Grid; (b) Voltage and current of load; (c) Voltage of Load and Parallel NPC Inverter currents; (d) PV array and Wind turbine current, Power and DC link voltages.

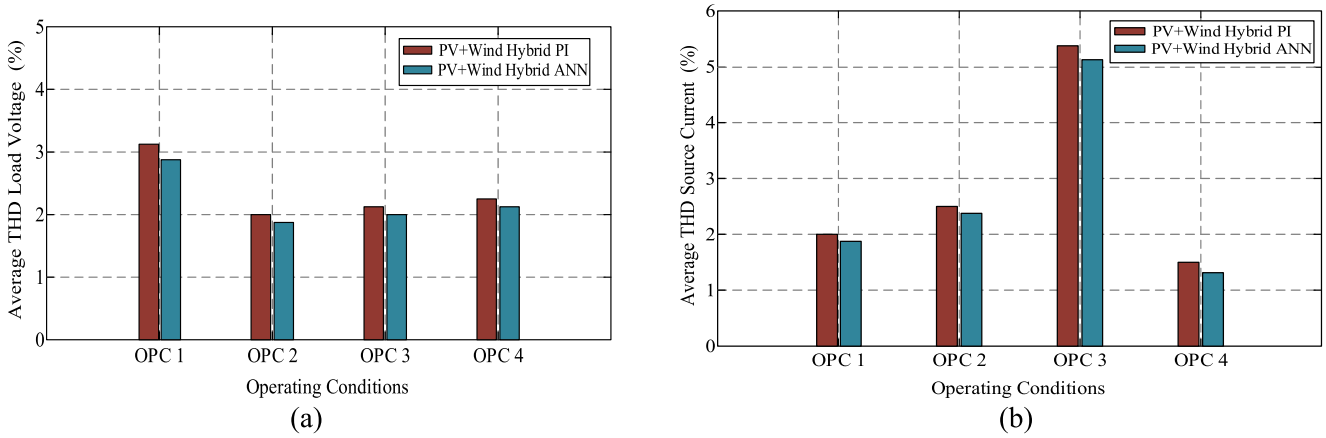

FIGURE 11. Performance of UPQC-ANN-RE System supplied by the hybrid PV-Wind power system using PI and ANN.

inject/dissipate power to/from the 3-Φ grid with great Power Factor.

Figure 11 shows performance of average THD of load voltage and source current on UPQC-ANN-RE system. Figure 11(a) shows that in OPC 1to 4, the employment of ANN on UPQC-ANN-RE system is capable to attain average THD of load voltage slightly better than PI controller and both method have already met the limit in IEEE 519. Figure 11(b) displays that in OPC 1 to 4, employment of ANN on UPQC-ANN-RE system is capable to attain average THD of source current slightly better than PI controller.

The waveforms of the dynamic outcomes of the UPQC-ANN-RE system for sudden changes in solar irradiance and wind speed, and load changes are shown in Figures 12 and 13. Figure 12 (a) and (b) displays voltage (v_{sa}) a current (i_{sa}) of grid at the PCC 1, voltage of load (v_{L_abc}) the PCC 2, and power of PV generator and wind turbine ($P_{pv-wind}$) during sudden change in solar irradiance and wind speed, taking into account operation with PI or ANN controllers, respectively. As can be seen, the UPQC-ANN-RE does active filtering only once the PV and wind system is inactive. Afterward, the UPQC-ANN-RE system delivers almost 3500 W of active power into the utility grid and load while wind turbines and PV are linked in conjunction with active filtering. Additionally, Figure 12(a) displays that the grid current dynamic response is slightly quicker than that shown in Figure 12(b) because of the usage of the ANN controller. Figure 13 (a) and (b) shows the simulation outcomes when load changes are made, e.g. 100% to 0% or 0% to 100%. The actual power spent by the load is about 740W, while the actual active power generated is about 3500W. As can be seen in Figure 13 (a) and (b), the power inserted in the utility grid rises when the load is disconnected. After the load is switched on again, the opposite occurs, the power inserted into the grid decreases. In this state the response of system is with ANN controller

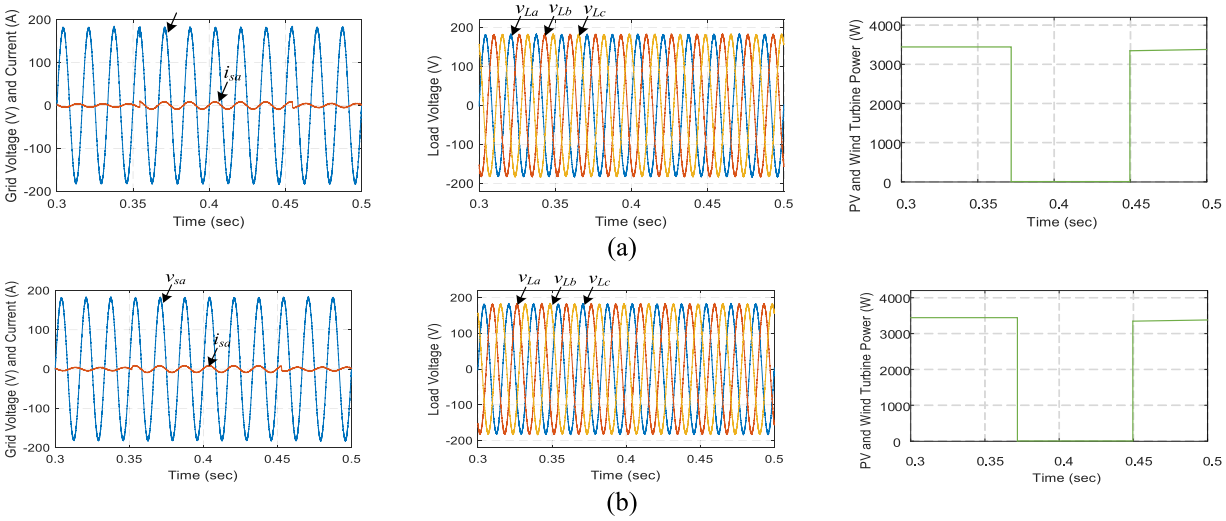

FIGURE 12. Sudden change in solar irradiance and wind speed: UPQC-ANN-RE performs active power insertion along with active filtering with $P_{pv-wind} > P_L$: (a) Sudden change in solar irradiance and wind speed with PI controller (100% to 0% and 0 % to 100 %): Phase "a" voltage and current of grid, voltage of load, and PV array and wind turbine power; (b) Sudden change in solar irradiance and wind speed with ANN controller (100% to 0% and 0 % to 100 %): Phase "a" voltage and current of grid, voltage of load, and PV array and wind turbine power.

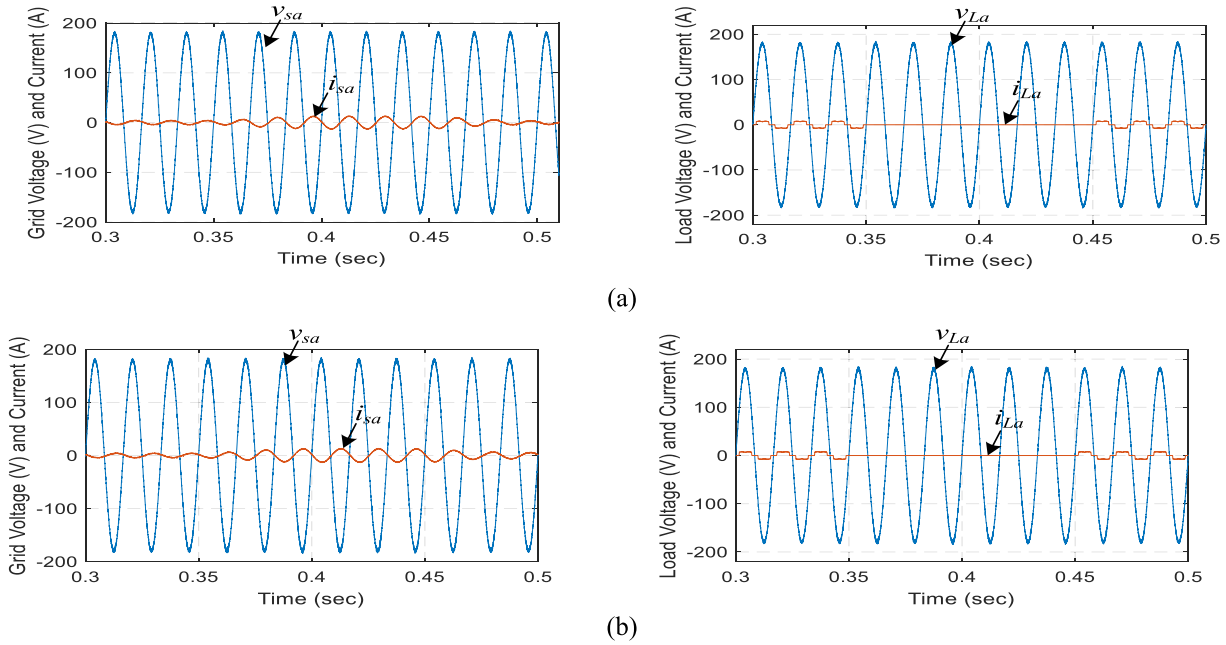

FIGURE 13. Sudden Load changes for OPC 4: UPQC-RE-ANN performs active power insertion along with active filtering with $P_{pv-wind} > P_L$: (a) sudden Load change (100 % to 0 % and 0% to 100%) with PI controller: Phase "a" voltage and current of grid, voltage and current of load; (b) sudden Load change (100 % to 0 % and 0% to 100%) with ANN controller: Phase "a" voltage and current of grid, voltage and current of load.

is slightly better as compared with PI. The average THD of load voltage in case of ANN controller is approximately 1.4% and with PI controller the average THD of load voltage is approximately 1.35%.

V. CONCLUSION

In this research work, a comparative performance analysis of a distributed generation system that integrates solar PV and wind power system using UPQC with ANN controller w.r.t PI controller is presented. So, steady state and dynamic analysis are done to assess and determine which controller would work best with UPQC. For this purpose, the simulation study was carried out using MATLAB to demonstrate the effectiveness of the proposed ANN based UPQC control system to improve the power quality of the hybrid PV-WT power system. To gauge the static performance, four operating conditions were considered, which comprising the voltages of grid, the features of the load and the energy generation of the photovoltaic and wind turbine (OPC 1-4). In contrast, the dynamic behaviors were assessed by considering the system

exposed to quick changes in solar insolation and wind speed, as well as load changes. The simulation outcomes illustrate that the UPQC-ANN-RE system attenuates the harmonics produced by the nonlinear load and is capable to attain average THD of the load and grid-side voltages and currents slightly improved than the PI controller, and each approach has already reached the limits of the IEEE-519 standard. Additionally, the system is able to perform an efficient power injection/dissipation to/from the grid with high Power Factor. The system also proves to be stable against fluctuations in irradiance and wind speed as well as load changes and reacts somewhat faster than the PI controller. It may be observed that the UPQC-ANN-RE system is able to do better series and parallel power line conditioning than PI, as well as supplying active power from PV and wind turbine arrangement. Therefore, UPQC-ANN-RE is a good way out for new distribution systems by integrating DGs with improving PQ.

REFERENCES

[1] J. Rocabert, A. Luna, F. Blaabjerg, and P. Rodríguez, "Control of power converters in AC microgrids," *IEEE Trans. Power Electron.*, vol. 27, no. 11, pp. 4734–4749, May 2012, doi: 10.1109/TPEL.2012.2199334.

[2] K. Sarita, S. Kumar, A. S. S. Vardhan, R. M. Elavarasan, R. K. Saket, G. M. Shafiullah, and E. Hossain, "Power enhancement with grid stabilization of renewable energy-based generation system using UPQC-FLC-EVA technique," *IEEE Access*, vol. 8, pp. 207443–207464, 2020, doi: 10.1109/ACCESS.2020.3038313.

[3] R. M. Elavarasan, "The motivation for renewable energy and its comparison with other energy sources: A review," *Eur. J. Sustain. Develop. Res.*, vol. 3, no. 1, pp. 1–19, Feb. 2019, doi: 10.20897/ejosdr/4005.

[4] D. Gielena, F. Boshella, D. Saygin, M. D. Bazilian, N. Wagner, and R. Gorini, "The role of renewable energy in the global energy transformation," *Energy Strategy Rev.*, vol. 24, pp. 38–50, Apr. 2019, doi: 10.1016/J.ESR.2019.01.006.

[5] M. M. Rahman, M. Shakeri, S. K. Tiong, F. Khatun, N. Amin, J. Pasupuleti, and M. K. Hasan, "Prospective methodologies in hybrid renewable energy systems for energy prediction using artificial neural networks," *Sustainability*, vol. 13, no. 4, pp. 1–28, 2021, doi: 10.3390/su13042393.

[6] N. Gupta and K. Seethalekshmi, "Artificial neural network and synchrosqueezing wavelet transform based control of power quality events in distributed system integrated with distributed generation sources," *Int. Trans. Electr. Energy Syst.*, vol. 31, no. 10, pp. 1–20, Oct. 2021, doi: 10.1002/2050-7038.12824.

[7] F. Z. Peng, "Editorial special issue on distributed power generation," *IEEE Trans. Power Electron.*, vol. 19, no. 5, pp. 1157–1158, Sep. 2004, doi: 10.1109/TPEL.2004.834801.

[8] E. J. Coster, J. M. A. Myrzik, B. Kruimer, and W. L. Kling, "Integration issues of distributed generation in distribution grids," *Proc. IEEE*, vol. 99, no. 1, pp. 28–39, Jan. 2011, doi: 10.1109/JPROC.2010.2052776.

[9] S. A. O. da Silva, L. B. G. Campanhol, G. M. Pelz, and V. de Souza, "Comparative performance analysis involving a three-phase UPQC operating with conventional and dual/inverted power-line conditioning strategies," *IEEE Trans. Power Electron.*, vol. 35, no. 11, pp. 11652–11665, Nov. 2020, doi: 10.1109/TPEL.2020.2985322.

[10] B. Singh, C. Jain, and S. Goel, "ILST control algorithm of single-stage dual purpose grid connected solar PV system," *IEEE Trans. Power Electron.*, vol. 29, no. 10, pp. 5347–5357, Oct. 2014, doi: 10.1109/TPEL.2013.2293656.

[11] R. K. Agarwa, I. Hussain, and B. Singh, "Three-phase single-stage grid tied solar PV ECS using PLL-less fast CTF control technique," *IET Power Electron.*, vol. 10, no. 2, pp. 178–188, Feb. 2017, doi: 10.1049/IET-PEL.2016.0067.

[12] Y. Singh, I. Hussain, B. Singh, and S. Mishra, "Single-phase solar grid-interfaced system with active filtering using adaptive linear combiner filter-based control scheme," *IET Gener. Transm. Distrib.*, vol. 11, no. 8, pp. 1976–1984, Jun. 2017, doi: 10.1049/IET-GTD.2016.1392.

[13] T.-F. Wu, H.-S. Nien, C.-L. Shen, and T.-M. Chen, "A single-phase inverter system for PV power injection and active power filtering with nonlinear inductor consideration," *IEEE Trans. Ind. Appl.*, vol. 41, no. 4, pp. 1075–1083, Jul. 2005, doi: 10.1109/TIA.2005.851035.

[14] G. M. Pelz, S. A. O. da Silva, and L. P. Sampaio, "Distributed generation integrating a photovoltaic-based system with a single- to three-phase UPQC applied to rural or remote areas supplied by single-phase electrical power," *Int. J. Electr. Power Energy Syst.*, vol. 117, May 2020, Art. no. 105673, doi: 10.1016/j.ijepes.2019.105673.

[15] A. Parida, S. Choudhury, and D. Chatterjee, "Microgrid based hybrid energy co-operative for grid-isolated remote rural village power supply for east coast zone of India," *IEEE Trans. Sustain. Energy*, vol. 9, no. 3, pp. 1375–1383, Jul. 2018, doi: 10.1109/TSTE.2017.2782007.

[16] F. M. D. Oliveira, S. A. O. da Silva, F. R. Durand, L. P. Sampaio, V. D. Bacon, and L. B. G. Campanhol, "Grid-tied photovoltaic system based on PSO MPPT technique with active power line conditioning," *IET Power Electron.*, vol. 9, no. 6, pp. 1180–1191, May 2016, doi: 10.1049/IET-PEL.2015.0655.

[17] L. B. G. Campanhol, S. A. O. da Silva, A. A. de Oliveira, and V. D. Bacon, "Dynamic performance improvement of a grid-tied PV system using a feed-forward control loop acting on the NPC inverter currents," *IEEE Trans. Ind. Electron.*, vol. 64, no. 3, pp. 2092–2101, Mar. 2017, doi: 10.1109/TIE.2016.2625779.

[18] L. B. G. Campanhol, S. A. O. da Silva, A. A. de Oliveira, and V. D. Bacon, "Single-stage three-phase grid-tied PV system with universal filtering capability applied to DG systems and AC microgrids," *IEEE Trans. Power Electron.*, vol. 32, no. 12, pp. 9131–9142, Dec. 2017, doi: 10.1109/TPEL.2017.2659381.

[19] *IEEE Power & Energy Society*, IEEE Standard 1459, 2010.

[20] L. B. G. Campanhol, S. A. O. da Silva, A. A. de Oliveira, and V. D. Bacon, "Power flow and stability analyses of a multifunctional distributed generation system integrating a photovoltaic system with unified power quality conditioner," *IEEE Trans. Power Electron.*, vol. 34, no. 7, pp. 6241–6256, Jul. 2019, doi: 10.1109/TPEL.2018.2873503.

[21] P. Ray, P. K. Ray, and S. K. Dash, "Power quality enhancement and power flow analysis of a PV integrated UPQC system in a distribution network," *IEEE Trans. Ind. Appl.*, vol. 58, no. 1, pp. 201–211, Jan. 2022, doi: 10.1109/TIA.2021.3131404.

[22] A. Reznik, M. G. Simões, A. Al-Durra, and S. M. Muyeen, "*LCL* filter design and performance analysis for grid-interconnected systems," *IEEE Trans. Ind. Appl.*, vol. 50, no. 2, pp. 1225–1232, Mar./Apr. 2014, doi: 10.1109/TIA.2013.2274612.

[23] J. He, Y. W. Li, F. Blaabjerg, and X. Wang, "Active harmonic filtering using current-controlled, grid-connected DG units with closed-loop power control," *IEEE Trans. Power Electron.*, vol. 29, no. 2, pp. 642–653, Feb. 2014, doi: 10.1109/TPEL.2013.2255895.

[24] G. M. Shafiullah, M. T. Arif, and A. M. T. Oo, "Mitigation strategies to minimize potential technical challenges of renewable energy integration," *Sustain. Energy Technol. Assessments*, vol. 25, pp. 24–42, Feb. 2018, doi: 10.1016/J.SETA.2017.10.008.

[25] L. Ashok Kumar and V. Indragandhi, "Power quality improvement of grid-connected wind energy system using facts devices," *Int. J. Ambient Energy*, vol. 41, no. 6, pp. 631–640, May 2020, doi: 10.1080/01430750.2018.1484801.

[26] A. M. Rauf and V. Khadkikar, "Integrated photovoltaic and dynamic voltage restorer system configuration," *IEEE Trans. Sustain. Energy*, vol. 6, no. 2, pp. 400–410, Apr. 2015, doi: 10.1109/TSTE.2014.2381291.

[27] S. A. Mohamed, "Enhancement of power quality for load compensation using three different FACTS devices based on optimized technique," *Int. Trans. Electr. Energy Syst.*, vol. 30, no. 3, Mar. 2020, Art. no. e12196, doi: 10.1002/2050-7038.12196.

[28] M. A. Mansor, K. Hasan, M. M. Othman, S. Z. B. M. Noor, and I. Musirin, "Construction and performance investigation of three-phase solar PV and battery energy storage system integrated UPQC," *IEEE Access*, vol. 8, pp. 103511–103538, 2020, doi: 10.1109/ACCESS.2020.2997056.

[29] S. Shetty, H. L. Suresh, M. Sharanappa, and C. H. V. Ramesh, "Performance of wind energy conversion system during fault condition and power quality improvement of grid-connected WECS by FACTS (UPFC)," in *Emerging Research in Computing, Information, Communication and Applications* (Advances in Intelligent Systems and Computing), vol. 906. 2019, pp. 211–225, doi: 10.1007/978-981-13-6001-5_16.

[30] S. Devassy and B. Singh, "Performance analysis of solar PV array and battery integrated unified power quality conditioner for microgrid systems," *IEEE Trans. Ind. Electron.*, vol. 68, no. 5, pp. 4027–4035, May 2021, doi: 10.1109/TIE.2020.2984439.

[31] A. Amirullah, A. Adiananda, O. Penangsang, and A. Soeprijanto, "Load active power transfer enhancement using UPQC-PV-BES system with fuzzy logic controller," *Int. J. Intell. Eng. Syst.*, vol. 13, no. 2, pp. 329–349, Apr. 2020, doi: 10.22266/IJIES2020.0430.32.

[32] Y. Bouzelata, E. Kurt, R. Chenni, and N. Altın, "Design and simulation of a unified power quality conditioner fed by solar energy," *Int. J. Hydrogen Energy*, vol. 40, no. 44, pp. 15267–15277, Nov. 2015, doi: 10.1016/J.IJHYDENE.2015.02.077.

[33] A. Amirullah, O. Penangsang, and A. Soeprijanto, "MATLAB/simulink simulation of unified power quality conditioner-battery energy storage system supplied by PV-wind hybrid using fuzzy logic controller," *Int. J. Electr. Comput. Eng.*, vol. 9, no. 3, pp. 1479–1495, 2019, doi: 10.11591/ijece.v9i3.pp1479-1495.

[34] M. Hosseinpou, A. Yazdian, M. Mohamadian, and J. Kazempour, "Design and simulation of UPQC to improve power quality and transfer wind energy to grid," *J. Appl. Sci.*, vol. 8, no. 21, pp. 3770–3782, Oct. 2008, doi: 10.3923/JAS.2008.3770.3782.

[35] S. Devassy and B. Singh, "Design and performance analysis of three-phase solar PV integrated UPQC," *IEEE Trans. Ind. Appl.*, vol. 54, no. 1, pp. 73–81, Jan. 2018, doi: 10.1109/TIA.2017.2754983.

[36] T. Lei, S. Riaz, N. Zanib, M. Batool, F. Pan, and S. Zhang, "Performance analysis of grid-connected distributed generation system integrating a hybrid wind-PV farm using UPQC," *Complexity*, vol. 2022, pp. 1–14, Mar. 2022.

[37] N. Zanib, M. Batool, S. Riaz, F. Afzal, S. Munawar, I. Daqqa, and N. Saleem, "Analysis and power quality improvement in hybrid distributed generation system with utilization of unified power quality conditioner," *Comput. Model. Eng. Sci.*, pp. 1–33, May 2022, doi: 10.32604/cmes.2022.021676.

[38] J. Jayachandran and R. M. Sachithanandam, "Performance investigation of unified power quality conditioner using artificial intelligent controller," *Int. Rev. Model. Simul.*, vol. 8, no. 1, pp. 48–56, Feb. 2015, doi: 10.15866/IREMOS.V8I1.5396.

[39] S. Sezen, A. Aktaş, M. Uçar, and E. Özdemir, "Design and operation of a multifunction photovoltaic power system with shunt active filtering using a single-stage three-phase multilevel inverter," *TURKISH J. Electr. Eng. Comput. Sci.*, vol. 25, pp. 1412–1425, 2017, doi: 10.3906/ELK-1602-381.

[40] R. A. Modesto, S. A. O. da Silva, and A. A. Júnior, "Power quality improvement using a dual unified power quality conditioner/uninterruptible power supply in three-phase four-wire systems," *IET Power Electron.*, vol. 8, no. 9, pp. 1595–1605, Sep. 2015, doi: 10.1049/IET-PEL.2014.0734.

[41] R. A. Modesto, S. A. O. da Silva, A. A. de Oliveira, and V. D. Bacon, "A versatile unified power quality conditioner applied to three-phase four-wire distribution systems using a dual control strategy," *IEEE Trans. Power Electron.*, vol. 31, no. 8, pp. 5503–5514, Aug. 2016, doi: 10.1109/TPEL.2015.2487867.

[42] B. W. França, L. F. da Silva, M. A. Aredes, and M. Aredes, "An improved iUPQC controller to provide additional grid-voltage regulation as a STATCOM," *IEEE Trans. Ind. Electron.*, vol. 62, no. 3, pp. 1345–1352, Mar. 2015, doi: 10.1109/TIE.2014.2345328.

[43] H. Fujita and H. Akagi, "The unified power quality conditioner: The integration of series- and shunt-active filters," *IEEE Trans. Power Electron.*, vol. 13, no. 2, pp. 315–322, Mar. 1998, doi: 10.1109/63.662847.

[44] V. D. Bacon and S. A. O. da Silva, "Performance improvement of a three-phase phase-locked-loop algorithm under utility voltage disturbances using non-autonomous adaptive filters," *IET Power Electron.*, vol. 8, no. 11, pp. 2237–2250, Nov. 2015, doi: 10.1049/IET-PEL.2014.0808.

[45] S. Vinnakoti and V. R. Kota, "ANN based control scheme for a three-level converter based unified power quality conditioner," *J. Electr. Syst. Inf. Technol.*, vol. 5, no. 3, pp. 526–541, Dec. 2018, doi: 10.1016/j.jesit.2017.11.001.

[46] M. Rahman, M. Shakeri, F. Khatun, S. K. Tiong, A. A. Alkahtani, N. A. Samsudin, N. Amin, J. Pasupuleti, and M. K. Hasan, "A comprehensive study and performance analysis of deep neural network-based approaches in wind time-series forecasting," *J. Reliable Intell. Environ.*, pp. 1–8, Jan. 2022, doi: 10.1007/s40860-021-00166-x.

[47] Z. Ming, W. Jian-Ru, W. Zhi-Qiang, and C. Jian, "Control method for power quality compensation based on Levenberg–Marquardt optimized bp neural networks," in *Proc. CES/IEEE 5th Int. Power Electron. Motion Control Conf.*, Feb. 2009, pp. 1–4, doi: 10.1109/IPEMC.2006.4778234.

[48] H. Yu, "Levenberg–Marquardt training," in *The Electronics Handbook*. Boca Raton, FL, USA: CRC Press, 2011. Accessed: Mar. 25, 2022. [Online]. Available: https://www.academia.edu/download/55871114/Levenberg-Marquardt.pdf

[49] J. J. Moré, "The Levenberg–Marquardt algorithm: Implementation and theory," in *Numerical Analysis*. Berlin, Germany: Springer, 1978, pp. 105–116, doi: 10.1007/BFB0067700.

NOOR ZANIB received the bachelor's and master's degrees in electrical engineering from the University of Engineering and Technology, Taxila (UET, Taxila), Taxila, Pakistan, in 2019 and 2022, respectively. Her research interests include smart grid, power electronics, power quality, and renewable energies.

MUNIRA BATOOL received the bachelor's degree in electrical engineering from Bahauddin Zakariya University, Multan, Pakistan, in 2007, the master's degree in electrical engineering from the University of Engineering and Technology, Taxila, Pakistan, in 2012, and the Ph.D. degree in electrical engineering from Curtin University. Her research interests include renewable energy resource modeling and integration in electrical power system networks, standalone, and clustered microgrids design for remote area networks with optimal operation.

SALEEM RIAZ was born in 1990. He received the B.S. degree in electrical engineering from the University of Engineering and Technology, Lahore, Punjab, Pakistan, in 2013, the M.S. degree in vehicle operation engineering from the School of Aeronautics, Northwestern Polytechnical University, in 2017, and the Ph.D. degree in electrical engineering from Northwestern Polytechnical University, Xi'an, in march 2022. His main research interest includes iterative learning control. His research interests also include: iterative learning for nonlinear dynamical control systems, optimal control theory, power electronics, motion control, robotics control, and control theory.

FAWAD NAWAZ received the bachelor's and master's degrees in electrical engineering from the University of Engineering and Technology, Taxila, Pakistan, in 2004 and 2009, respectively. He is currently pursuing the Doctor of Engineering degree with the Engineering Institute of Technology, Perth, Australia. His research interests include modern power system operation and their control strategies.